

Associations Between Capillary Diameter, Capillary Density, and Microaneurysms in Diabetic Retinopathy: A High-Resolution Confocal Microscopy Study

Dong An^{1,2}, Riley Pulford^{1,2}, William H. Morgan^{1,2}, Dao-Yi Yu^{1,2}, and Chandrakumar Balaratnasingam¹⁻³

¹ Centre for Ophthalmology and Visual Science, University of Western Australia, Perth, Australia

² Lions Eye Institute, Nedlands, Western Australia, Australia

³ Department of Ophthalmology, Sir Charles Gairdner Hospital, Western Australia, Australia

Correspondence: Dao-Yi Yu, Centre for Ophthalmology and Visual Science, The University of Western Australia, Nedlands, Western Australia 6009, Australia. e-mail: dyyu@lei.org.au

Received: May 20, 2020

Accepted: October 11, 2020

Published: February 9, 2021

Keywords: retina; microaneurysm; capillary; diabetes; macula

Citation: An D, Pulford R, Morgan WH, Yu D-Y, Balaratnasingam C. Associations between capillary diameter, capillary density, and microaneurysms in diabetic retinopathy: A high-resolution confocal microscopy study. *Trans Vis Sci Tech.* 2021;10(2):6. <https://doi.org/10.1167/tvst.10.2.6>

Purpose: To use high-resolution histology to define the associations between microaneurysms, capillary diameter and capillary density alterations in diabetic retinopathy (DR).

Methods: Quantitative comparisons of microaneurysm number, capillary density and capillary diameter were performed between eight human donor eyes with nonproliferative DR and six age- and eccentricity-matched normal donor eyes after retinal vascular perfusion labelling. The parafovea, 3-mm, 6-mm, and 9-mm retinal eccentricities were analyzed and associations between microvascular alterations defined.

Results: Mean capillary density was reduced in all retina regions in the DR group ($P = 0.013$). Microaneurysms occurred in all retina regions in the DR group, but the association between decreased capillary density and microaneurysm number was only significant in the 3-mm ($P = 0.040$) and 6-mm ($P = 0.007$) eccentricities. The mean capillary diameter of the DR group ($8.9 \pm 0.53 \mu\text{m}$) was greater than the control group ($7.60 \pm 0.40 \mu\text{m}$; $P = 0.033$). There was no association between capillary diameter increase and capillary density decrease ($P = 0.257$) and capillary diameter increase and microaneurysm number ($P = 0.147$) in the DR group. Within the parafovea of the DR group, capillary density was significantly reduced, and capillary diameter was significantly increased in the deep capillary plexus compared with the superficial and intermediate plexuses (all $P < 0.05$).

Conclusions: In DR, capillary density reduction occurs across multiple retina eccentricities with a predilection for the deep capillary plexus. The association between microaneurysm number and capillary density is specific to retina eccentricity. Capillary diameter increase may be an early biomarker of DR. These findings may refine the application of optical coherence tomography angiography techniques for the management of DR.

Introduction

Microvascular alterations are the hallmark feature of diabetic retinopathy (DR).¹⁻⁵ Although the previous pathologic studies by Ashton,^{2,6,7} Ballantyne and Loewenstein,³ Cogan et al.,¹ Kuwabara,¹ and others^{5,8-10} have provided critical insights into the histologic changes that characterize DR, there remains a dearth of information regarding the associations between the varying retinal capillary abnormalities.

Microaneurysm formation,^{8,11,12} regional capillary density decrease,^{5,13-16} and, more recently, capillary diameter increase, are measurable biomarkers that have been used to detect DR.^{5,17-19} However, the interrelationships between these microstructural alterations are yet to be clearly defined. This situation has posed limitations on our understanding of the temporality and pathogenic links in DR. The nonuniform patterns of microangiopathy and the predilection of distinct retinal eccentricities and capillary plexuses to vascular injury in DR have also not been clarified in depth.

Table 1. Donor Demographic Information

Eye Number	Diabetes	Age	Sex	Cause of Death
1	Y	58	M	Alcoholism/acute pancreatitis
2	Y	70	M	Severe diabetic complications of multiple organ systems
3	Y	45	F	Severe diabetic vascular complications/sepsis
4	Y	70	M	Ischemic cardiomyopathy
5	Y	70	M	Ischemic cardiomyopathy
6	Y	66	M	Acute myocardial infarction
7	Y	82	M	Acute myocardial infarction
8	Y	82	M	Acute myocardial infarction
9	N	89	F	Intracranial hemorrhage
10	N	60	M	Leukemia
11	N	75	F	Endometrial carcinoma
12	N	75	F	Endometrial carcinoma
13	N	71	M	Acute myocardial infarction
14	N	85	F	Lung carcinoma

Eyes No. 4 and 5, 7 and 8, 11 and 12 were obtained from single donors.

These are important pathobiologic concepts that have potential applications for disease screening, stratifying disease severity, and prognosticating visual outcomes.

The state of the art of retinal vascular disease management is shifting toward the application of optical coherence tomography angiography (OCTA) techniques to detect disease-induced structural vascular alterations.^{15,20–22} A major advantage of OCTA is the capacity to resolve retinal capillaries, the predominant site of early vascular injury in DR, with greater reproducibility and precision than dye-based angiographic techniques.^{23–26} Technology refinement has also improved visualization of the retinal vasculature within the peripheral retina in addition to the posterior pole.^{27–29} OCTA techniques can, therefore, be leveraged to detect the very earliest stages of DR, before ophthalmoscopically evident retinal changes manifest.^{11,13,30,31} Quantitative histologic studies that define the order, magnitude, and type of microvascular alterations that occur in DR as well as delineating any variations that are specific to retinal eccentricity will greatly inform the application of such technology.

We present a high-resolution confocal microscopy study that focusses on three microvascular abnormalities that characterize DR: microaneurysms, capillary density decrease, and capillary diameter increase.^{8,17,18,20,32–34} Using age-matched normal donor tissue we quantify the microvascular changes per retinal eccentricity and capillary plexus in eyes with DR after perfusion labelling³⁵ with endothelial antibodies. Associations between the three microvascular abnormalities are subsequently delineated. This report serves several purposes: (1) to provide quanti-

tative histologic data that can be used to improve the application of OCTA techniques to detect and quantify DR and (2) to refine our understanding of the pathophysiologic mechanisms underlying DR and to speculate on the biologic connections between the different microvascular alterations.

Materials and Methods

The study was approved by the human research ethics committee at the University of Western Australia. All human tissue was handled according to the Tenets of the Declaration of Helsinki.

Donor Eyes

Fourteen human eyes from 11 donors were used. All eyes were obtained from DonateLife WA, the organ and tissue retrieval authority in Western Australia, or the Lions Eye Bank, Lions Eye Institute, Western Australia, Australia. Specimens obtained via the Lions Eye Bank were posterior segments only following removal of the cornea for transplantation purposes. The demographic details and cause of death for all donors are presented in Table 1.

The donor cohort in this study was stratified into a control group and DR group. The control group included eyes with no history of eye disease and no history of diabetes mellitus. The DR group included eyes from donors that, upon medical record review, were confirmed to have a diagnosis of type 2 diabetes

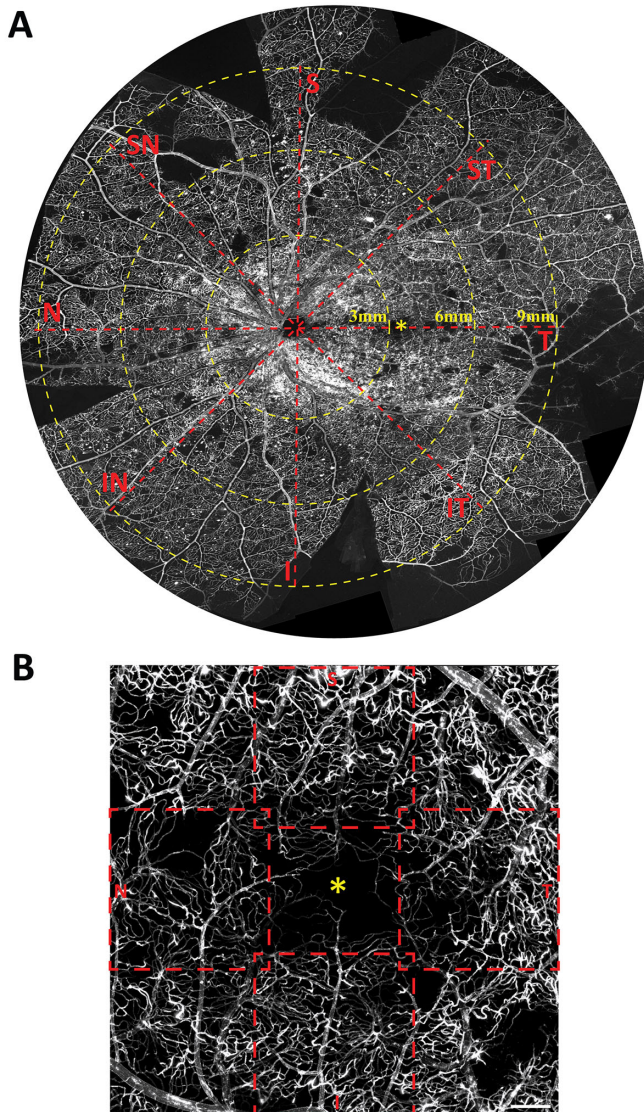


Figure 1. Whole-mount histologic image of a diabetic donor retina labelled with lectin-FITC illustrates the retina regions that were studied (A). The superimposed grid is centered on the optic disc. Confocal Z-stacks of 1.24 mm × 1.24 mm were sampled at each 3-mm, 6-mm, and 9-mm eccentricities in eight directions. The parafovea region (B) was sampled in four separate locations – superior, temporal, inferior and nasal to the foveal avascular zone (*). I, inferior; IN, inferonasal; IT, inferotemporal; N, nasal; S, superior; SN, superonasal; ST, superotemporal; T, temporal. Scale bar = 300 μm.

mellitus and were treated with oral antiglycemic agents and/or insulin. Only those eyes that demonstrated the histologic vascular alterations that characterize DR, such as microaneurysms, capillary nonperfusion, retinal hemorrhage, and intraretinal microvascular abnormalities as seen on flat mount fluorescent microscopy, were included in this study.^{1,2} Eyes from donors with diabetes mellitus that did not demonstrate features of DR on postmortem microscopic examination were not included in the study. Additionally, tissue

that was deemed to be of poor quality such that it was not possible to perform confocal imaging and reliable quantitative histologic analysis was excluded from this study.

Tissue Preparation

All donor eyes were obtained within 12 hours of death. Enucleated eyes were transported in Ringers lactate solution that had been bubbled with a mixture of 5% CO₂/95% O₂. At the laboratory, the eye was placed in a custom-built eye holder and the portion of the central retinal artery, before it traversed the optic nerve sheath inferiorly, was identified and dissected free of retro-orbital fat under the operating microscope. Our method of microcannulation and perfusion-based labelling techniques was then used to label the vascular endothelium of the retinal microvasculature.^{24,36,37} Eyes were cannulated using a glass micropipette (100–150 μm tip diameter), and subsequently perfused with 1% bovine serum albumin dissolved in Ringer's lactate solution to wash out residual blood clots. Perfusion fixation was achieved with a solution of 4% paraformaldehyde for 20 minutes followed by 0.1 M phosphate buffer wash for 15 minutes. Eyes from all donors were perfused with 0.02 mg lectin-fluorescein isothiocyanate (FITC, Sigma-Aldrich, Product No. L4895 Darmstadt, Germany) in 0.4 mL of phosphate buffer by slow push over 30 seconds to label the luminal endothelium. After 12 minutes, the eye was perfused again with phosphate buffer for 15 minutes to washout excess labels. The perfusate for all eyes also contained 1 μg Hoechst (Sigma-Aldrich Product No. H6024) for nuclear labelling.

After perfusion, the eye was decannulated and dissected along the equator. The vitreous was carefully peeled from the retina. The posterior segment was then immersed in 4% paraformaldehyde for 12 hours. Next, the neuro-retina was detached from the retinal pigment epithelium. The optic nerve head was sectioned to be continuous with the retina. The retina was flat mounted by making several radial incisions along the edge. Glycerol (MERCK Pty. Limited, Victoria, Australia) was added to enhance the optical quality of the tissue before placement of the coverslip.

Confocal Scanning Laser Microscopy

After cannulation and perfusion of the central retinal artery, all orders of the retinal microvasculature were examined to ensure complete perfusion and washout of blood from the retinal vasculature. In all specimens, the flat-mount was imaged in a standardized manner using the optic disk as the reference point

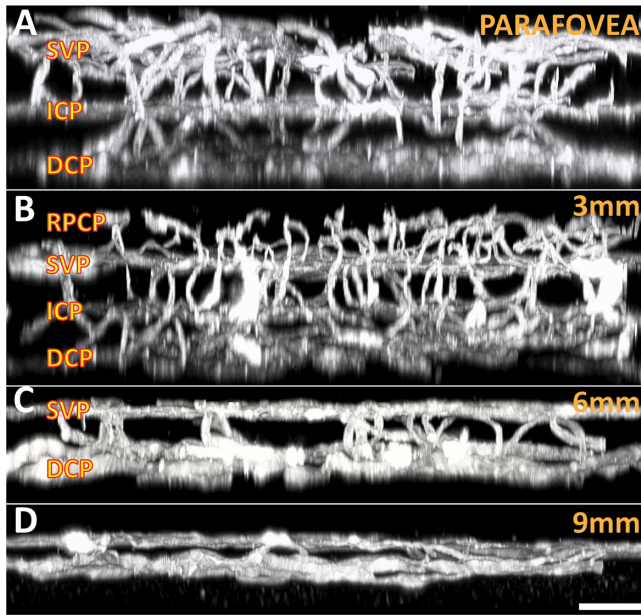


Figure 2. Three-dimensional organization of capillary networks at different eccentricities. The parafovea (A) consists of three separate plexuses, including the SVP, ICP, and DCP. The 3-mm location (B) along each of the vascular arcades also contains an additional layer—the retinal peripapillary capillary plexus (RPCP). The retina thins peripherally, where the 6-mm region (C) typically contains two distinct retinal layers, with arteries and veins running within the superficial layer. The 9-mm region (D) typically contains only a single capillary plexus, with large vessels located in a slightly more superficial plane. Scale bar = 60 μm .

(Fig. 1A). Specifically, images were acquired using a confocal scanning laser microscope (Nikon Eclipse 90i, Nikon Corporation, Tokyo, Japan) and a Nikon 10 \times NA 0.45 dry objective lens with a field of view of 1.27 mm \times 1.27 mm and 1- μm Z-intervals. The locations included 3 mm, 6 mm, and 9 mm measured from the center of the optic disc in eight directions 45 $^\circ$ apart, namely superior, superotemporal, temporal, inferotemporal, inferior, inferonasal, nasal and superonasal (Fig. 1A). Because the 3-mm temporal location corresponded with the foveal avascular zone, it was not sampled. Instead, the macula region was sampled in four different locations: superior, nasal, inferior, and temporal to the foveal avascular zone (Fig. 1B), located within the perimeters of the parafovea according to Hogan’s definition.³⁸ A total of 11 posterior pole locations, 8 midperiphery locations, and 8 periphery locations were sampled. A sampling location was omitted if it was at a site of incision for flat-mounting purpose.

Lectin-FITC labelling was visualized using 488-nm argon laser excitation with emissions detected through 515-nm band pass filters. Simultaneous scanning was done in each donor eye to visualize the nuclei using

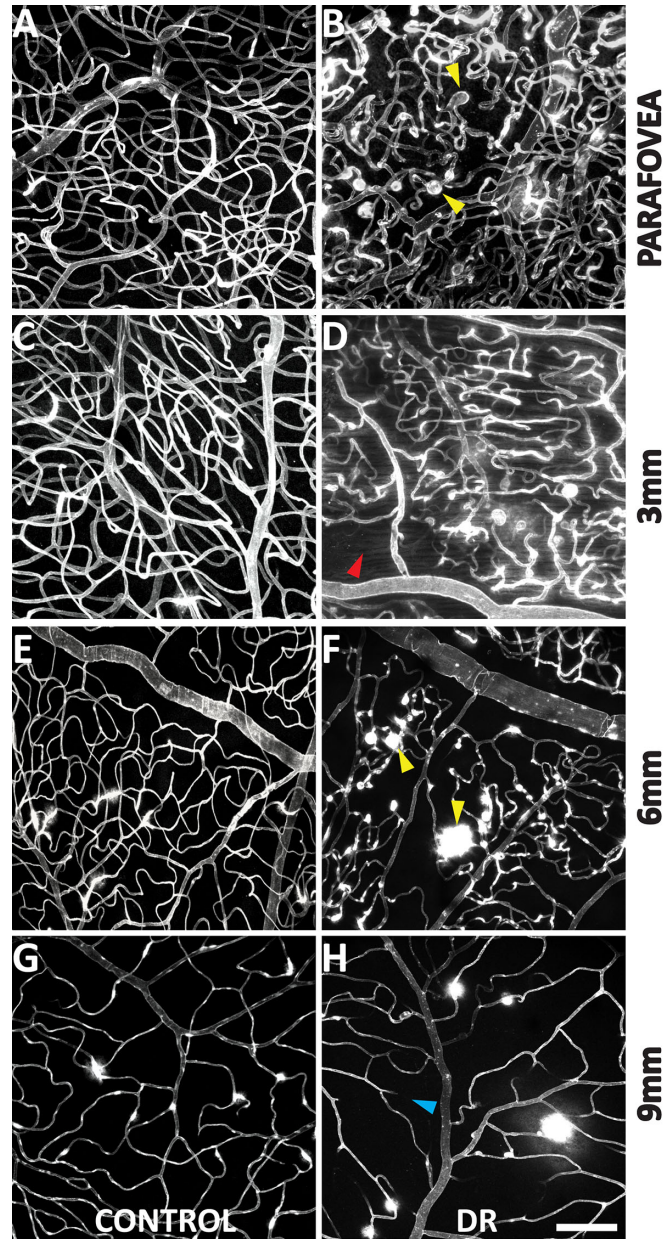


Figure 3. Capillary density comparison between control and DR groups at each retina location. Each image depicts a Z-projection of all capillary plexuses of a full thickness confocal microscopy stack. Capillary density was significantly less in the 3-mm and 6-mm locations in the DR group. Microaneurysms are indicated in panels B and F (yellow arrows). Panel D highlights an area of capillary dropout (red arrow). Panel H (blue arrow) highlights an occluded retinal vessel. Scale-bar = 100 μm .

408 nm argon laser excitation with emissions detected through a 450-nm band pass filter. All images in this manuscript were prepared using Adobe Photoshop CS4 (Version 12.1, Adobe Systems Inc., Mountain View, CA) and Adobe Illustrator CS5 (version 15.1.0, Adobe Systems Inc.).

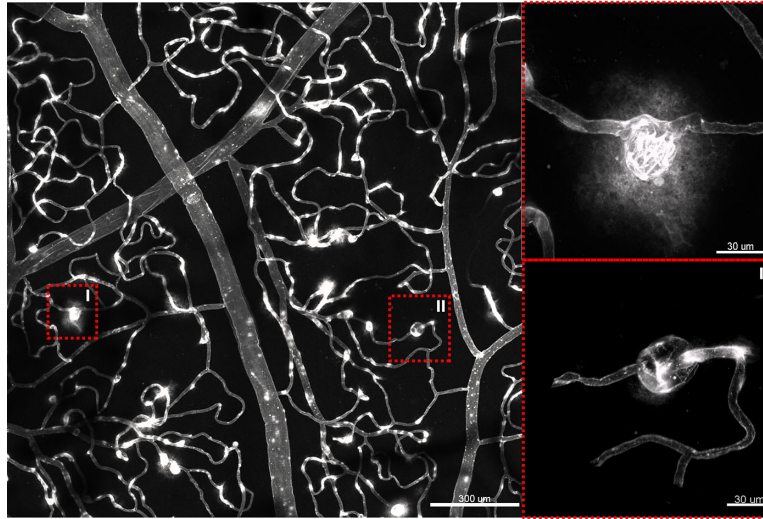


Figure 4. Leakage of lectin-FITC at the site of microaneurysms. Insets provide magnified views of two microaneurysms in the 9-mm eccentricity. Note that there is leakage associated with the microaneurysm in Inset I as seen by hyperfluorescence beyond the vascular wall. There is no leakage associated with the microaneurysm in inset II. Both of these microaneurysms are saccular in morphology and measure 30 μm in diameter.

Image Analysis

Confocal microscopy image files were processed with IMARIS (Bitplane, Zurich, Switzerland). Image preparation was performed by D.A. Quantifications of capillary density and capillary diameter were performed by R.P (blinded). The following parameters were quantified:

1. Capillary density—Capillary density was counted for each plexus of each retinal eccentricity. For the parafoveal locations and 3-mm locations, capillary density was counted for the superficial vascular plexus (SVP), the intermediate capillary plexus (ICP), and deep capillary plexus (DCP) and the combined capillary density. For the 3-mm locations, the retinal peripapillary capillaries, if present, were counted as part of the SVP. For the 6-mm locations, the densities of the SVP and DCP were calculated. For the 9-mm locations, a single plexus was calculated. Segmentation was performed within IMARIS guided by co-localization of nuclei to vascular staining and by three-dimensional visualization of the stack.^{5,23,25} The SVP extend from the inner limiting membrane to the outer border of the ganglion cell layer. The ICP extend from the border of ganglion cell layer/inner nuclear layer to the middle one-half of the inner nuclear layer. The DCP extend from the middle one-half of

the inner nuclear layer to the outer border of the outer plexiform layer.³⁹ After segmentation, a two-dimensional projected image was formed from the three-dimensional stack using the “IMARIS Easy 3D function.” Using our previously published methods,^{39–42} a 3×3 grid was drawn on each of the two-dimensional images and the number of capillaries intersected by the grids were manually counted (Supplementary Fig. S1) to represent the relative capillary density in a $1.24 \text{ mm} \times 1.24 \text{ mm}$ field.

2. Capillary diameter—The blinded observer was instructed to select 10 capillaries evenly and randomly from each study location. Chosen capillaries were measured at approximately midpoint along their courses, away from bifurcations and away from bulges, which indicate the sites of endothelial nuclei. A line was drawn perpendicular to the capillary between the endothelium walls to measure the luminal diameter of the capillary.^{5,42} Individual measurements were combined to calculate mean capillary diameter and standard deviation for the location. For all eccentricities other than the parafovea, measurements were obtained from full thickness three-dimensional projected images. For parafoveal locations, measurements were obtained for each of the plexuses: the SVP, the ICP, and the DCP as described in the capillary density section.

3. Microaneurysm frequency—For all images, the number of microaneurysms was manually defined and counted. This goal was achieved by scrolling through the entire confocal volume to study each slice and by generating three-dimensional images of the entire confocal volume using Imaris software and studying the image at varying angles of rotation. We adopted the histologic criteria previously described by Ashton,⁶ Ballantyne and Loewenstein,³ and Cogan et al.¹ to define a microaneurysm and differentiate it from a normal capillary, a retinal hemorrhage, and abnormal staining patterns. Specifically, microaneurysms were defined as the outpouching of the wall of a capillary segment within any capillary plexus that was more than 20 μm across the widest diameter.

Statistical Analysis

Data were analyzed using R (A language and environment for statistical computing. R Foundation for Statistical Computing, Vienna, Austria; www.R-project.org/). Statistical calculations were performed using linear mixed models using eye number (identity) and right/left eye as the random effects, to address the correlation between multiple sampling regions within the same eye, as well as between the eyes obtained from the same donor. The following analyses were performed for all regions and each of the four eccentricities including the parafovea, 3 mm, 6 mm, and 9 mm from the center of the optic disc:

1. Association of capillary density (response variable) and diagnosis (control vs. DR). The DR group was further subdivided. If a 1.24 mm \times 1.24 mm field did not contain a microaneurysm, it was designated as the DRMA– group. If the field contained at least one microaneurysm, it was designated as the DRMA+ group. Comparisons between the control, DRMA–, and DRMA+ groups were performed using linear mixed models. A subanalysis comparing the SVP+ICP, and DCP of the parafovea was also performed.
2. Association of capillary diameter (response variable) and diagnosis (control vs. DR). As above, the DR group was further divided into DRMA– and DRMA+ groups. A subanalysis comparing the SVP+ICP and DCP of the parafovea was also performed.

The following analyses were performed only within the DR group:

1. Association of capillary density (response variable) and the number of microaneurysms.
2. Association of capillary density (response variable) and capillary diameter.
3. Association of capillary diameter (response variable) and the number of microaneurysms.

The normality of capillary density and diameter data was determined using Shapiro Wilk normality test and visualized using q–q norm plots.

Results

Eight eyes with DR from six donors with diabetes mellitus and six control eyes from five normal donors were analyzed. Patient demographic information can be found in [Table 1](#). All donors were of Caucasian ancestry. The mean age for the DR group was 67.9 ± 12.2 years. The mean age for the control group was 75.8 ± 10.3 years and was not significantly different from the DR group ($P = 0.101$). There was no record of ophthalmic care for any of the donors. Premortem clinical imaging data were not available, and there was no evidence of laser photocoagulation scars in any of the donor retinas upon examination with microscopy.

Qualitative Analysis

The three-dimensional arrangement of capillary plexuses in each of the retina eccentricities is illustrated in [Figure 2](#). The parafoveal region was composed of three capillary plexuses including the SVP, ICP, and DCP ([Fig. 2A](#)). The 3-mm region located at the superotemporal, superonasal, inferotemporal, and inferonasal directions were composed of four capillary plexuses ([Fig. 2B](#)). The additional plexus is the retinal peripapillary capillary plexus, which radiates from the optic disc peripherally along the vascular arcades.^{5,43–45} The superior, temporal, inferior, and nasal 3-mm regions were composed of three plexuses. The 6-mm sampling region was composed of two capillary plexuses—a superficial and a deep plexus ([Fig. 2C](#)). The 9-mm region was composed of only a single capillary plexus and the arteries and veins were seen to be located at a slightly more superficial plane compared with the capillary network ([Fig. 2D](#)).

Projections of the entire confocal volume to present a two-dimensional image of all capillary plexuses in the parafovea, 3-mm region, 6-mm region, and 9-mm region in control and DR groups are provided in [Figure 3](#). Eyes with DR demonstrated observable

Table 2. Comparison of Capillary Densities of Control versus DR

Region	Plexus	Control Mean Capillary Density	DR Mean Capillary Density	DR vs. Control Capillary Density Change	DR vs. Control P Value	DR Eyes With Lower Density Than Control (n = 8)
Parafovea	SVP	41.4 ± 9.5	43.5 ± 11.7	5.1%	0.479	37.50%
	ICP	47.1 ± 10.8	44.3 ± 11.8	-5.9%	0.360	50%
	DCP	38.8 ± 6.5	20.6 ± 17.8	-46.9%	<0.001	87.50%
	Combined	127.6 ± 11.1	104.5 ± 18.8	-18.1%	0.001	100%
3 mm	SVP	45.5 ± 12.9	42.0 ± 15.3	-7.7%	0.249	50%
	ICP	45.3 ± 9.4	39.3 ± 14.1	-13.2%	0.017	75%
	DCP	26.4 ± 8.3	15.9 ± 14.2	-39.8%	<0.001	87.50%
	Combined	119.8 ± 10.1	91.5 ± 24.3	-23.6%	<0.001	87.50%
6 mm	SVP	43.1 ± 12.1	33.9 ± 11.3	-21.3%	<0.001	100%
	DCP	41.2 ± 8.4	31.2 ± 14.2	-24.3%	<0.001	100%
	Combined	88.4 ± 9.1	64.9 ± 15.7	-26.6%	<0.001	100%
9 mm	One plexus	57.1 ± 14.8	44.0 ± 11.3	-22.9%	<0.001	87.50%

Data from combined and individual plexuses are presented. Combined capillary densities were calculated using full thickness retinal projections; therefore, they may slightly differ from the sum of densities of individual plexuses.

decreases in capillary density at varying retinal eccentricities. The vessel walls in eyes with DR frequently demonstrated greater staining than control eyes (Fig. 4). Microaneurysms were seen in all eyes with DR. The endothelium of microaneurysms were typically hyperfluorescent compared with the adjacent capillaries. We also observed significant extravascular leakage of FITC at the site of some microaneurysms (Fig. 4; Inset I), whereas other microaneurysms did not demonstrate any leakage (Fig. 4; Inset II).

Quantitative Analysis

Capillary Density and Capillary Diameter Comparisons between the Control and DR Groups

Capillary density and capillary diameter were not associated with age and sex for both the control group and DR group (all $P > 0.05$).

Capillary Density

When measurements of all retinal plexuses/eccentricities were analyzed, mean capillary density of the DR group (74.8 ± 33.8) was significantly less than the control group (93.5 ± 34.8 ; $P = 0.013$). Analysis by region revealed a significantly lower mean capillary density in the DR group in the parafovea (104.5 ± 18.8 vs. 127.6 ± 21.1 ; $P = 0.001$), 3-mm (91.5 ± 24.3 vs. 119.8 ± 10.1 ; $P < 0.001$), 6-mm (64.9 ± 15.7 vs. 88.4 ± 9.1 ; $P < 0.001$) and 9-mm (44.0 ± 11.3 vs. 57.1 ± 14.8 ; $P < 0.001$) retinal eccentricities (Table 2).

Parafovea. Morphologies of the parafoveal SVP, ICP, and DCP are illustrated in Figure 5. Comparison within the control group revealed a denser ICP (47.1 ± 10.8) than SVP (41.4 ± 9.5 ; $P < 0.001$). Both the SVP and ICP are denser than the DCP (38.8 ± 6.5 ; $P = 0.017$ and $P = 0.045$, respectively). Comparison within the DR group showed no significant difference between the ICP (44.3 ± 11.8) and SVP (43.5 ± 11.7 ; $P = 0.564$) and both ICP/SVP were denser than the DCP (18.0 ± 6.6). Comparisons between the control and DR groups showed similar SVP density (41.4 ± 9.5 vs. 43.5 ± 11.7 ; $P = 0.479$) and ICP density (47.1 ± 10.8 vs. 44.3 ± 11.8 ; $P = 0.360$). The DCP of control group was significantly denser than DR group (38.8 ± 6.5 vs. 18.0 ± 6.6 ; $P < 0.001$).

The 3-mm Location. For the control group, the density of the SVP (45.5 ± 12.9) was similar to that of the ICP (44.5 ± 9.4 ; $P = 0.443$). Both the SVP and ICP were denser than the DCP (29.9 ± 8.3 ; both $P < 0.001$). For the DR group, the density of the SVP (41.0 ± 15.3) was similar to that of the ICP (38.3 ± 14.1 ; $P = 0.091$). Both the SVP and the ICP were denser than the DCP (14.9 ± 14.2 ; both $P < 0.001$). A comparison between the control and DR groups revealed no difference in SVP density (45.4 ± 12.9 vs. 41.0 ± 15.3 ; $P = 0.249$), a decrease in the ICP density (44.5 ± 9.4 vs. 38.3 ± 14.1 ; $P = 0.017$), and a decrease in the DCP density (29.9 ± 8.3 vs. 14.9 ± 14.2 ; $P < 0.001$) in DR group.

The 6-mm Location. For the control group, there was no significant difference between the densities of the SVP

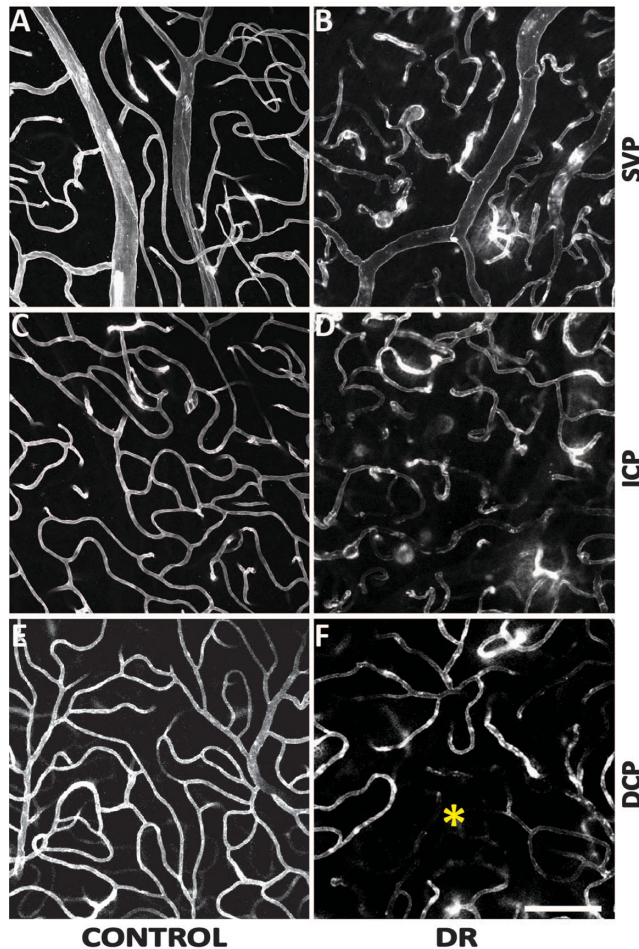


Figure 5. Comparisons of the parafoveal vasculature between control and DR groups. The SVP (A and B), ICP (C and D), and the DCP (E and F) were presented. Capillary diameters were increased in the DR group across all three plexuses. Capillary density was seen to be decreased in the DCP in the DR group where an area of impaired capillary perfusion was noted (*). Scale bar = 100 μ m.

(46.1 ± 12.1) and the DCP (43.2 ± 8.4 ; $P = 0.113$). Similarly, for the DR group, there was no significant difference between the SVP (34.9 ± 11.3) and the DCP (31.2 ± 14.2 ; $P = 0.226$). Comparison between the groups revealed a significantly decreased density of the SVP (46.1 ± 12.1 vs. 34.9 ± 11.3 ; $P < 0.001$) and DCP (43.2 ± 8.4 vs. 31.2 ± 14.2 ; $P < 0.001$) in the DR group.

The density of each DR eye at each region was compared with the mean density of controls.

Eyes 1, 4, and 6 recorded greatest density decrease in the 6-mm region (a decrease of 60.7%, 67.1%, and 17.6%, respectively). Eyes 2, 5, 7, and 8 recorded greatest density decrease in the 9-mm region (a decrease of 40.6%, 33.7%, 34.4%, and 55.2%, respectively). Only eye 3 recorded a large density decrease at the 3-mm region by 178.6%. Overall, 7 of the 8 eyes had a greater more density decrease in the peripheral areas than posterior pole areas.

Capillary Diameter

The mean capillary diameter was $7.60 \pm 0.40 \mu$ m for the control group versus $8.9 \pm 0.53 \mu$ m for the DR group ($P = 0.033$) (Supplementary Fig. S2). In the control group, there was no significant difference in the mean capillary diameter between the parafovea ($7.37 \pm 0.4 \mu$ m), 3-mm ($7.35 \pm 0.41 \mu$ m), and 6-mm ($7.36 \pm 0.32 \mu$ m) regions (all $P > 0.05$). The 9-mm region had a mean capillary diameter of $8.50 \pm 0.33 \mu$ m that was significantly greater than the other regions (all $P < 0.05$). In the DR group, the 3-mm location ($9.49 \pm 0.92 \mu$ m) had a significantly larger mean capillary diameter than the other three regions (parafovea: $8.83 \pm 1.34 \mu$ m; 6 mm: $8.67 \pm 0.87 \mu$ m; 9 mm: $8.74 \pm 1.30 \mu$ m; all $P < 0.01$). There was no significant difference found between these three regions (all $P > 0.05$).

The DR group had a significantly greater capillary diameter in the 3-mm ($9.49 \pm 0.70 \mu$ m vs. $7.36 \pm 0.53 \mu$ m; $P = 0.010$) and parafovea ($8.83 \pm 0.60 \mu$ m vs. $7.38 \pm 0.45 \mu$ m; $P = 0.031$) regions compared with the control group. The capillary diameter in the 6-mm and 9-mm regions did not significantly differ between the groups ($P = 0.240$).

In the control group, the capillaries in the parafoveal DCP were smaller in diameter compared with both capillaries of the SVP ($6.88 \pm 1.21 \mu$ m; $P < 0.001$) and ICP ($6.65 \pm 1.11 \mu$ m; $P = 0.012$). There was no significant difference between the SVP and ICP ($P = 0.423$). In the DR group, the capillaries in the parafoveal DCP were larger in diameter compared with the ICP ($9.23 \pm 1.37 \mu$ m vs. $8.21 \pm 1.03 \mu$ m; $P = 0.007$). No significant difference was found between the SVP ($9.12 \pm 0.89 \mu$ m) and DCP ($P = 0.234$), and between the SVP and ICP ($P = 0.071$). Comparing each of the plexuses between the two groups, the SVP, ICP, and DCP of the DR group all had significantly larger capillary diameters than the controls ($P = 0.003$; $P = 0.012$; $P = 0.002$, respectively).

For capillary density and capillary diameter analyses, the DR group was further stratified into two groups: (1) sampling fields without microaneurysm (DRMA-) and (2) sampling fields with at least one microaneurysm (DRMA+). All three groups in all four regions (parafovea, 3 mm, 6 mm, and 9 mm) were compared and the results are summarized in Table 3 and Figure 6. The mean capillary density measurements of all capillary plexuses in the DRMA- group were not different from the control group ($P = 0.480$), but had a significantly higher density than the DRMA+ group ($P < 0.001$). The mean capillary diameter measurements in all regions in the DRMA- and DRMA+ were similar ($P = 0.420$) and both had a

Table 3. Regression Analyses for Capillary Density and Capillary Diameter Across All Regions

	Group Comparison	Capillary Density	SE	P Value	Capillary Diameter (μm)	SE	P Value
All regions	C vs. DRMA–	93.5 vs. 87.9	8.1	0.480	7.6 vs. 8.8	0.5	0.029
	C vs. DRMA+	93.5 vs. 64.8	7.8	<0.001	7.6 vs. 9.0	0.6	0.012
	DRMA– vs. DRMA+	87.9 vs. 64.8	5.2	<0.001	8.8 vs. 9.0	0.3	0.420
Parafovea	C vs. DRMA–	127.6 vs. 105.3	21.1	0.024	7.4 vs. 8.8	0.6	0.025
	C vs. DRMA+	127.6 vs. 102.9	12.5	0.031	7.4 vs. 9.0	0.6	0.170
	DRMA– vs. DRMA+	105.3 vs. 102.9	9.1	0.793	8.8 vs. 9.0	0.4	0.585
3 mm	C vs. DRMA–	119.8 vs. 106.5	11.9	0.266	7.4 vs. 8.7	0.9	0.170
	C vs. DRMA+	119.8 vs. 81.9	11.5	0.001	7.4 vs. 10.0	0.8	0.005
	DRMA– vs. DRMA+	106.5 vs. 81.9	6.9	0.001	8.7 vs. 10.0	0.9	0.163
6 mm	C vs. DRMA–	88.4 vs. 80.3	9.0	0.375	7.4 vs. 8.7	0.7	0.091
	C vs. DRMA+	88.4 vs. 58.3	8.2	<0.001	7.4 vs. 8.8	0.7	0.075
	DRMA– vs. DRMA+	80.3 vs. 58.1	6.0	<0.001	8.7 vs. 8.8	0.5	0.961
9 mm	C vs. DRMA–	57.1 vs. 45.0	7.2	0.097	8.5 vs. 8.9	0.7	0.635
	C vs. DRMA+	57.1 vs. 41.8	7.0	0.033	8.5 vs. 8.3	0.9	0.844
	DRMA– vs. DRMA+	45.0 vs. 41.8	4.6	0.487	8.9 vs. 8.3	0.8	0.513

For each region, the control group, DR group with no microaneurysm, and DR group with microaneurysm were compared using linear mixed modelling. The 3-mm, 6-mm, and 9-mm regions indicate distance from the center of the optic disc. Capillary density indicates the number of capillary intercepts with a 3×3 grid laid over a $1.27 \text{ mm} \times 1.27 \text{ mm}$ field. Mixed effect used for linear mixed modelling = right/left eye nested within donor identity. SE, standard error; C, control; DRMA–, DR group with no microaneurysm in sampling field; DRMA+, DR group with microaneurysm in sampling field.

significantly larger capillary diameter than the control group ($P = 0.029$; $P = 0.012$, respectively). 0.031 ± 0.019 , $P = 0.031$; and 9 mm, 0.038 ± 0.018 , $P = 0.018$).

Microaneurysm Frequency in DR

Microaneurysms were present in all DR eyes and not present in any of the controls. The DR group had a mean of 2.9 ± 5.7 microaneurysms per sampling field of $1.24 \text{ mm} \times 1.24 \text{ mm}$. Within the DR group, the 6-mm (4.58 ± 8.0) and 3-mm (3.43 ± 5.86) regions both had significantly higher numbers of microaneurysms than the parafovea (0.69 ± 1.47 ; $P_{3\text{-mm}} = 0.025$; $P_{6\text{-mm}} = 0.001$). The 6-mm region also had a greater frequency of microaneurysms than the 9-mm region (1.69 ± 2.65 ; $P = 0.006$). Other regional comparisons were not significantly different. The SVP of the parafovea had a mean of 0.15 ± 0.67 microaneurysms per field. The ICP had a mean of 0.17 ± 0.77 microaneurysms per field. The DCP had a mean of 0.09 ± 0.39 microaneurysms per field. There was no significant difference between the SVP/ICP ($P = 0.544$), SVP/DCP ($P = 0.082$), and ICP/DCP ($P = 0.113$).

The mean microaneurysm count to capillary density ratio for all regions was 0.039. The 6-mm region had the highest ratio of 0.070 ± 0.019 (Fig. 7). The microaneurysm count to capillary density ratio of the 6-mm region was significantly higher than all other three regions (parafovea, 0.007 ± 0.021 , $P = 0.001$; 3 mm,

Association Between Capillary Density and Microaneurysm Frequency in DR

Data from all regions were pooled. Capillary density was negatively associated with the number of microaneurysms (intercept = 77.5; slope = -1.0 ; $P = 0.015$). Specifically, microaneurysms were more frequent at sites of lower capillary density. A subanalysis revealed that the association was significant at the 3-mm (intercept = 96.2; slope = -1.4 ; $P = 0.040$) and 6-mm (intercept = 69.1; slope = -0.961 ; $P = 0.007$) regions (Fig. 8). However, analysis of the parafovea (intercept = 109.8; slope = -7.7 ; $P = 0.051$) and 9-mm (intercept = 41.2; slope = 0.68; $P = 0.408$) regions did not reveal a significant association.

Association Between Capillary Diameter and Microaneurysm Frequency in DR

Pooled data showed no association between capillary diameter and microaneurysm frequency in the DR group ($P = 0.147$).

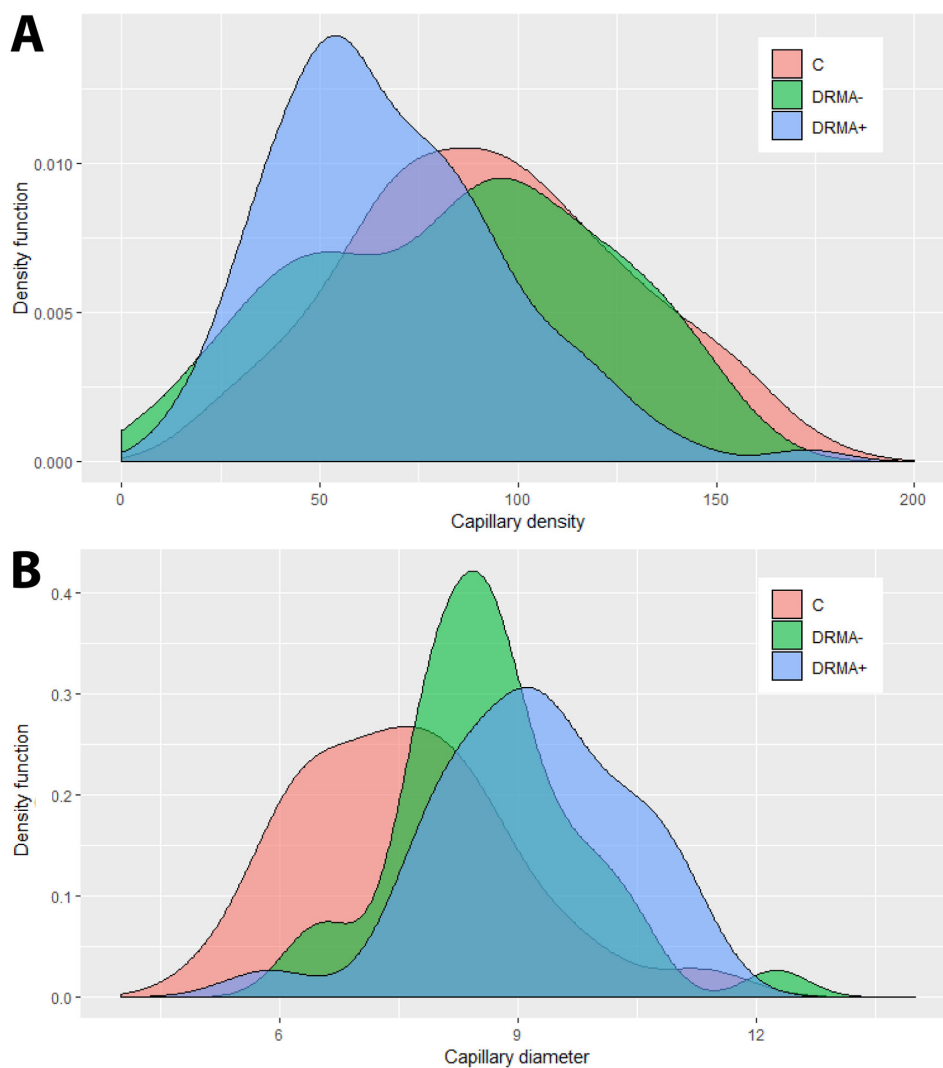


Figure 6. The distribution of capillary density (**A**) and capillary diameter (**B**) across the three groups—controls (**C**), DRMA⁻, and DRMA⁺ were plotted with density functions. For capillary density, the control group and the DRMA⁻ group show similar distribution whereas the DRMA⁺ group has a significantly lower capillary density. For capillary diameter, the control group had a significantly lower diameter than both DR groups. Capillary diameter of the DRMA⁺ group was not statistically different from the DRMA⁻ group, but graphically, an observable trend can be seen that capillary widening occurs more frequently in the DRMA⁺ group.

Association Between Capillary Density and Capillary Diameter in DR

Pooled data showed no association between capillary density and capillary diameter in the DR group ($P = 0.257$).

Discussion

This article defines the histologic relationships between capillary density, capillary diameter and microaneurysm frequency in DR. The major findings are as follows.

1. Capillary density reduction is a hallmark feature of DR that occurs in multiple retina eccentricities with a predilection for the DCP.
2. Microaneurysm number is modulated by regional capillary density.
3. Capillary diameter can be increased in regions of DR eyes without presence of microaneurysms.

Retinal ischemia owing to microvascular occlusion is an established pathogenic factor in DR.^{2,46,47} Tok Bek performed a histopathologic analysis of 12 donor eyes from patients with diabetes mellitus following perfusion vascular casting and described varying degrees of vascular closure ranging from focal loss

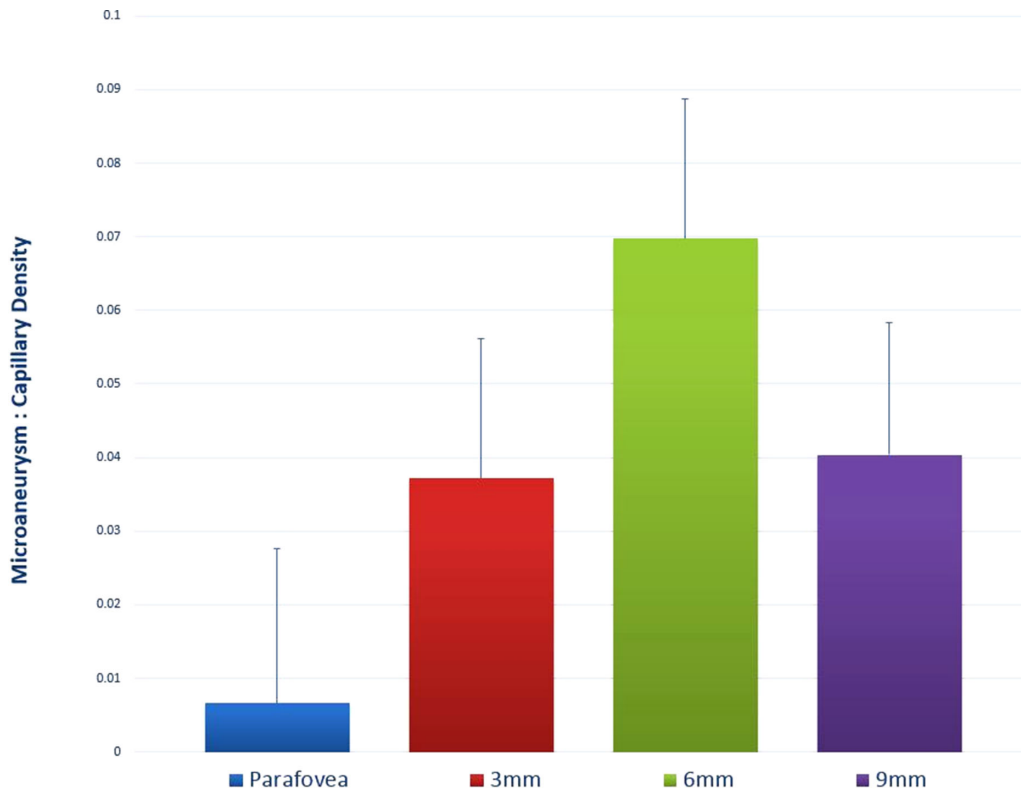


Figure 7. Associations between microaneurysms and capillary density. The microaneurysm to capillary density ratio was plotted for each of the four study regions. A higher ratio indicates a higher relative frequency of microaneurysms, taking into account the variations in normal capillary density between different retina eccentricities.

of capillaries to diffuse nonperfusion secondary to arteriolar occlusion.^{48,49} Studies using rodent models of diabetes have shown that microvascular occlusions within the retina are largely composed of activated leukocytes and monocytes.⁵⁰ Progressive capillary closure can lead to the development of macular edema and retinal neovascularization by initiating the biochemical cascades involved in angiogenesis.⁵¹ A recognition of microvascular occlusion is, therefore, vital in mitigating the development of these sight-threatening complications. Quantifying retinal vascular density is a useful means of detecting microvascular occlusion, however, this can be difficult as it is a parameter that varies with age and retinal eccentricity in normal eyes.^{52,53} In this report we used age-matched and eccentricity-matched control tissue to account for these confounding variables. By using such an approach, we demonstrate that retinal capillary density is not decreased focally, but involves many eccentricities throughout the retina in DR. Our findings thereby support the use of a panretinal ischemic index derived using ultrawide field fluorescein angiography or OCTA for detecting and determining the severity of DR.^{27,29}

Microaneurysms are pathologic dilatations of the capillary wall and a frequent manifestation of DR.^{2,8,54} Wise proposed that retinal microaneurysms represent abortive attempts of retinal neovascularization and correlate to sites of tissue anoxia/hypoxia.^{55,56} This was consequent to the observations by Cogan et al., whom noted that microaneurysms predominantly occur at the border of, and orientate toward, capillaries that are devoid of endothelia.¹ In our study, we were able to demonstrate a significant and negative association between microaneurysm count and capillary density thereby reaffirming the postulations of previous authors.^{1,2,8,9} However, importantly, our quantitative analysis demonstrates that the relationship between capillary density and microaneurysm number is modulated by retinal eccentricity. Specifically, microaneurysm number was inversely related to capillary density in the 3-mm and 6-mm regions only; this relationship was not significant in the parafovea and 9-mm eccentricity. There are several plausible explanations for this observed nonuniform relationship. (1) The lack of association found at the parafovea ($P = 0.051$) may be due to a limitation of four sampling locations compared with eight sampling

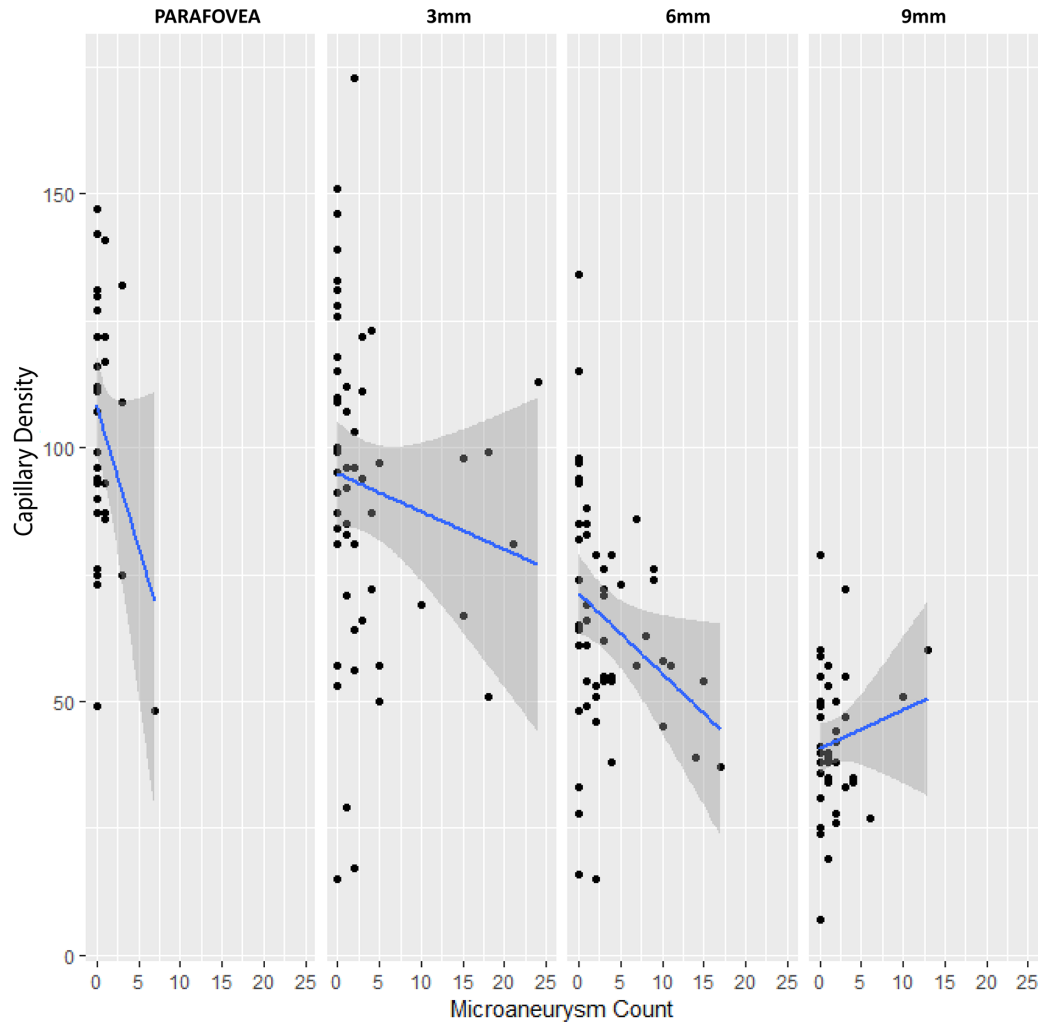


Figure 8. Capillary density was plotted against microaneurysm count in each of the four study regions. A regression line was fitted for each region. Both the 3-mm ($P = 0.040$) and 6-mm ($P = 0.007$) regions had significant associations between microaneurysm number and capillary density. The parafovea region exhibited a steep regression line, however, the association did not reach statistical significance ($P = 0.051$). In the 9-mm region, capillary density was also not associated with microaneurysm frequency ($P = 0.408$).

locations at the 3-mm, 6-mm, and 9-mm locations. A very steep slope was observed for the parafovea region (Fig. 8). The parafoveal region may demonstrate a significant association between density and microaneurysm number with a larger sample size. (2) Enzymes involved in mitochondrial energy production such as neuroglobin and cytochrome oxidase as well as glia populations are abundant in the parafovea.^{57,58} These nonvascular mechanisms may, therefore, confer the parafovea some degree of protection from energy depletion after capillary loss. (3) Because retina thickness is relatively lower in the 9-mm eccentricity,⁵⁹ neurons at this site may receive some oxygenation from the choroidal circulation and protect against tissue hypoxia after retinal capillary loss. We emphasize that these are speculations and that further work is required

to clarify the relationship between capillary density and microaneurysm number in DR.

Our recent report demonstrated that nonproliferative DR is associated with a mean increase in capillary diameter by almost 35% in the peripapillary region.⁵ Similarly, in this study we found that mean capillary diameter was increased in the DR group (8.9 μm) compared with the control group (7.6 μm). Disruption of the blood–retina barrier (BRB) is one of the most critical pathogenic factors in DR and plays a putative role in the formation of microaneurysms, retinal hemorrhage, and loss of retina capillaries.⁶⁰ However, in this study we failed to find an association between capillary diameter and microaneurysm number or capillary diameter and capillary density changes, suggesting that pathogenic mechanisms other

than BRB breakdown may be responsible for capillary diameter increase. It is plausible that an increase in the capillary diameter reflects perturbations in neurovascular coupling or activation of neurodegenerative mechanisms within the retina. For example, extracellular glutamate is increased in short-term experimental DR.⁶¹ An increase in glutamate-mediated signaling can in turn lead to the release of nitric oxide from neurons and arachidonic acid derivatives from the glia with a net effect of capillary dilation.⁶² Our data also lead us to conclude that capillary diameter increases might be an early feature of DR before the onset of BRB breakdown. Specifically, we found that capillary diameter was significantly greater than control eyes at sites where capillary density changes and microaneurysm formation did not occur. Our postulations regarding the sequence of change in DR are consistent with affirmations that neurodegeneration may precede BRB breakdown^{63–65}; however, further histologic studies are required in this area.

The parafovea is a highly specialized region of the human retina that is the site of greatest retinal ganglion cell density.⁶⁶ The unique metabolic demands of neuroglial cells in the parafovea are satisfied by the distinct, layered organization of capillary plexuses that is topologically different from many other retina eccentricities.⁶⁷ The pathogenesis of DR has an uneven influence on the circulatory beds of the parafovea with a predilection for the DCP, as shown in a number of OCTA studies.^{30,32} Few studies, however, have performed a stratified histologic analysis of the human macular circulation to confirm these clinical observations. The histopathology in this study validates and supports the affirmations of previous authors; we demonstrate that the capillary density in the DR group is preferentially decreased in the DCP of the parafovea. This finding is consistent with our previous histologic analysis of the peripapillary region that also showed a significant decrease in the DCP in DR.⁵ In this study, we also demonstrate that the mean capillary diameter increase in the DR group was greater in the DCP than in the SVP and ICP. The reason for the preferential vulnerability of the DCP to injury in DR remains unclear. The sequestration of inflammatory cells and microvascular occlusion of capillaries is a proposed mechanism,⁶⁸ but our findings do not support this hypothesis alone because the mean diameter of the DCP was significantly greater than the SVP and ICP in DR. Several reasons may account for the increased vulnerability of the DCP: (1) The DCP is located adjacent to the outer plexiform layer, a layer of high oxygen consumption during physiologic states^{69,70}; and (2) The DCP's lack of regulatory capability in response to changes in systemic blood pressure.⁷¹

Although we were unable to elucidate the mechanisms underlying these changes, the findings in this report highlight the importance of precise clinical imaging of the DCP as a means of detecting the early features of DR.

This study provides important histologic correlates that may refine the clinical management of DR. Owing to the rapid escalation in technology development, the resolving power of OCTA devices has improved to 2 to 4 μm in the axial plane allowing capture of the range of capillary abnormalities described in this report.⁷² Although microaneurysms are an early biomarker of DR, they are not always readily visualized using OCTA owing to the absence of flow within the lumen of some aneurysms.²⁶ The findings in this report suggest that retinal capillary diameter measurements may be a better surrogate marker of early DR than microaneurysms. The capacity of OCTA to stratify the parafoveal circulation, with special reference to the DCP, also makes it a powerful tool in the early detection of DR.^{73,74}

We acknowledge several limitations of this study namely the limited sample size of donor eyes as well as the lack of premortem clinical information from *Diabetes* donors to correlate with the histologic results. In addition, the number of microaneurysms identified using current perfusion labelling methodology may be an underestimate, as only microaneurysms with patent lumens can be labelled. Finally, we did not examine the pericytes and, therefore, were unable to define the important relationships between pericytes and the spectrum of microvascular changes described in this study.

Acknowledgments

The authors thank staff from the Lions Eye Bank of Western Australia, Lions Eye Institute, for provision of human donor eyes and staff from DonateLife WA, the Western Australian agency for organ and tissue donation who facilitated the recruitment of donors into the study by referral and completion of consent processes.

Supported by the Investigator Grant of National Health and Medical Research Council of Australia (APP1173403) and a priming grant from the Raine Medical Research Foundation.

Disclosure: **D. An**, None; **R. Pulford**, None; **W.H. Morgan**, None; **D.-Y. Yu**, None; **C. Balaratnasingam**, Novartis, Roche, Allergan, Bayer (C)

References

1. Cogan DG, Toussaint D, Kuwabara T. Retinal vascular pattern. IV diabetic retinopathy. *Arch Ophthalmol*. 1961;66:366–378.
2. Ashton N. Studies of the retinal capillaries in relation to diabetic and other retinopathies. *Br J Ophthalmol*. 1963;47:521–538.
3. Ballantyne AJ, Loewenstein A. Retinal microaneurysms and punctate haemorrhages. *Br J Ophthalmol*. 1944;28:593–598.
4. Yanoff M. Ocular pathology of diabetes mellitus. *Am J Ophthalmol*. 1969;67:21–38.
5. An D, Chandrasekera E, Yu DY, Balaratnasingam C. Non-proliferative diabetic retinopathy is characterized by non-uniform alterations to peripapillary capillary networks. *Invest Ophthalmol Vis Sci*. 2020;61:39.
6. Ashton N. Vascular changes in diabetes with particular reference to the retinal vessels; preliminary report. *Br J Ophthalmol*. 1949;33:407–420.
7. Ashton N. Vascular basement membrane changes in diabetic retinopathy. Montgomery lecture, 1973. *Br J Ophthalmol*. 1974;58:344–366.
8. Stitt AW, Gardiner TA, Archer DB. Histological and ultrastructural investigation of retinal microaneurysm development in diabetic patients. *Br J Ophthalmol*. 1995;79:362–367.
9. Garner A. Histopathology of diabetic retinopathy in man. *Eye (Lond)*. 1993;7(Pt 2):250–253.
10. Bresnick GH, Davis MD, Myers FL, de Venecia G. Clinicopathologic correlations in diabetic retinopathy. II. Clinical and histologic appearances of retinal capillary microaneurysms. *Arch Ophthalmol*. 1977;95:1215–1220.
11. Yang JY, Wang Q, Yan YN, et al. Microvascular retinal changes in pre-clinical diabetic retinopathy as detected by optical coherence tomographic angiography. *Graefes Arch Clin Exp Ophthalmol*. 2020;258:513–520.
12. Spencer T, Phillips RP, Sharp PF, Forrester JV. Automated detection and quantification of microaneurysms in fluorescein angiograms. *Graefes Arch Clin Exp Ophthalmol*. 1992;230:36–41.
13. Cao D, Yang D, Huang Z, et al. Optical coherence tomography angiography discerns preclinical diabetic retinopathy in eyes of patients with type 2 diabetes without clinical diabetic retinopathy. *Acta Diabetol*. 2018;55:469–477.
14. Chu Z, Lin J, Gao C, et al. Quantitative assessment of the retinal microvasculature using optical coherence tomography angiography. *J Biomed Opt*. 2016;21:66008.
15. Hwang TS, Zhang M, Bhavsar K, et al. Visualization of 3 distinct retinal plexuses by projection-resolved optical coherence tomography angiography in diabetic retinopathy. *JAMA Ophthalmol*. 2016;134:1411–1419.
16. Kogachi K, Lin TC, Palejwala NV, et al. Quantitative assessment of changes in retinal vascular density and morphology among patients with diabetic retinopathy using spectral domain optical coherence tomography angiography (SD-OCTA). *Invest Ophthalm Vis Sci*. 2018;59:2665–1561.
17. Burns SA, Elsner AE, Chui TY, et al. In vivo adaptive optics microvascular imaging in diabetic patients without clinically severe diabetic retinopathy. *Biomed Opt Express*. 2014;5:961–974.
18. Chui TY, Pinhas A, Gan A, et al. Longitudinal imaging of microvascular remodelling in proliferative diabetic retinopathy using adaptive optics scanning light ophthalmoscopy. *Ophthalmic Physiol Opt*. 2016;36:290–302.
19. Lombardo M, Parravano M, Serrao S, Ducoli P, Stirpe M, Lombardo G. Analysis of retinal capillaries in patients with type 1 diabetes and nonproliferative diabetic retinopathy using adaptive optics imaging. *Retina*. 2013;33:1630–1639.
20. Lee J, Rosen R. Optical coherence tomography angiography in diabetes. *Curr Diab Rep*. 2016;16:123.
21. Nesper PL, Roberts PK, Onishi AC, et al. Quantifying microvascular abnormalities with increasing severity of diabetic retinopathy using optical coherence tomography angiography. *Invest Ophthalmol Vis Sci*. 2017;58: BIO307–BIO315.
22. Balaratnasingam C, Inoue M, Ahn S, et al. Visual acuity is correlated with the area of the foveal avascular zone in diabetic retinopathy and retinal vein occlusion. *Ophthalmology*. 2016;123:2352–2367.
23. Balaratnasingam C, An D, Freund KB, Francke A, Yu DY. Correlation between histologic and OCT angiography analysis of macular circulation. *Ophthalmology*. 2019;126:1588–1589.
24. An D, Balaratnasingam C, Heisler M, et al. Quantitative comparisons between optical coherence tomography angiography and matched histology in the human eye. *Exp Eye Res*. 2018;170:13–19.
25. Balaratnasingam C, An D, Sakurada Y, et al. Comparisons between histology and optical coherence tomography angiography of the periarterial capillary-free zone. *Am J Ophthalmol*. 2018;189:55–64.
26. Schreur V, Domanian A, Liefers B, et al. Morphological and topographical appearance of microaneurysms on optical coherence tomography angiography. *Br J Ophthalmol*. 2018;103:630–635.

27. Ehlers JP, Jiang AC, Boss JD, et al. Quantitative ultra-widefield angiography and diabetic retinopathy severity: an assessment of panretinal leakage index, ischemic index and microaneurysm count. *Ophthalmology*. 2019;126:1527–1532.
28. Zhang QQ, Chen CL, Chu ZD, Attaran-Rezaei K, Wang RKK. Ultra-wide field optical coherence tomography angiography for evaluation of diabetic retinopathy. *Invest Ophthalmol Vis Sci*. 2017;58:5447.
29. Silva PS, Cavallerano JD, Sun JK, Soliman AZ, Aiello LM, Aiello LP. Peripheral lesions identified by mydriatic ultrawide field imaging: distribution and potential impact on diabetic retinopathy severity. *Ophthalmology*. 2013;120:2587–2595.
30. Furino C, Montrone G, Cicinelli MV, et al. Optical coherence tomography angiography in diabetic patients without diabetic retinopathy. *Eur J Ophthalmol*. 2020;30:1418–1423.
31. Sacconi R, Casaluci M, Borrelli E, et al. Multimodal imaging assessment of vascular and neurodegenerative retinal alterations in type 1 diabetic patients without fundoscopic signs of diabetic retinopathy. *J Clin Med*. 2019;8:1409.
32. Kaizu Y, Nakao S, Arima M, et al. Capillary dropout is dominant in deep capillary plexus in early diabetic retinopathy in optical coherence tomography angiography. *Acta Ophthalmol*. 2019:e812.
33. Dupas B, Minvielle W, Bonnin S, et al. Association between vessel density and visual acuity in patients with diabetic retinopathy and poorly controlled type 1 diabetes. *JAMA Ophthalmol*. 2018;136:721–728.
34. Kaizu Y, Nakao S, Yoshida S, et al. Optical coherence tomography angiography reveals spatial bias of macular capillary dropout in diabetic retinopathy. *Invest Ophthalmol Vis Sci*. 2017;58:4889–4897.
35. Yu DY, Su EN, Cringle SJ, Yu PK. Isolated preparations of ocular vasculature and their applications in ophthalmic research. *Prog Retin Eye Res*. 2003;22:135–169.
36. Yu PK, Balaratnasingam C, Morgan WH, Cringle SJ, McAllister IL, Yu DY. The structural relationship between the microvasculature, neurons, and glia in the human retina. *Invest Ophthalmol Vis Sci*. 2010;51:447–458.
37. Yu PK, McAllister IL, Morgan WH, Cringle SJ, Yu DY. Inter-relationship of arterial supply to human retina, choroid, and optic nerve head using micro perfusion and labeling. *Invest Ophthalmol Vis Sci*. 2017;58:3565–3574.
38. Hogan MJ, Alvarado JA, Weddell JE. *Histology of the Human Eye: An Atlas and Textbook*. Philadelphia: W.B. Saunders Company; 1971.
39. Chan G, Balaratnasingam C, Yu PK, et al. Quantitative morphometry of perifoveal capillary networks in the human retina. *Invest Ophthalmol Vis Sci*. 2012;53:5502–5514.
40. Tan PE, Yu PK, Balaratnasingam C, et al. Quantitative confocal imaging of the retinal microvasculature in the human retina. *Invest Ophthalmol Vis Sci*. 2012;53:5728–5736.
41. Chan G, Balaratnasingam C, Yu PK, et al. Quantitative changes in perifoveal capillary networks in patients with vascular comorbidities. *Invest Ophthalmol Vis Sci*. 2013;54:5175–5185.
42. Chandrasekera E, An D, McAllister IL, Yu DY, Balaratnasingam C. Three-dimensional microscopy demonstrates series and parallel organization of human peripapillary capillary plexuses. *Invest Ophthalmol Vis Sci*. 2018;59:4327–4344.
43. Henkind P. Radial peripapillary capillaries of the retina. I. Anatomy: human and comparative. *Br J Ophthalmol*. 1967;51:115–123.
44. Yu PK, Balaratnasingam C, Xu J, et al. Label-free density measurements of radial peripapillary capillaries in the human retina. *PLoS One*. 2015;10:e0135151.
45. Yu PK, Cringle SJ, Yu DY. Correlation between the radial peripapillary capillaries and the retinal nerve fibre layer in the normal human retina. *Exp Eye Res*. 2014;129:83–92.
46. Curtis TM, Gardiner TA, Stitt AW. Microvascular lesions of diabetic retinopathy: clues towards understanding pathogenesis? *Eye (Lond)*. 2009;23:1496–1508.
47. Engerman RL. Pathogenesis of diabetic retinopathy. *Diabetes*. 1989;38:1203–1206.
48. Bek T. Transretinal histopathological changes in capillary-free areas of diabetic retinopathy. *Acta Ophthalmol (Copenh)*. 1994;72:409–415.
49. Bek T. A clinicopathological study of venous loops and reduplications in diabetic retinopathy. *Acta Ophthalmol Scand*. 2002;80:69–75.
50. Schroder S, Palinski W, Schmid-Schonbein GW. Activated monocytes and granulocytes, capillary nonperfusion, and neovascularization in diabetic retinopathy. *Am J Pathol*. 1991;139:81–100.
51. Miller JW, Adamis AP, Shima DT, et al. Vascular endothelial growth-factor vascular-permeability factor is temporally and spatially correlated with ocular angiogenesis in a primate model. *Am J Pathol*. 1994;145:574–584.
52. Sato R, Kunikata H, Asano T, et al. Quantitative analysis of the macula with optical coherence

- tomography angiography in normal Japanese subjects: the Taiwa study. *Sci Rep*. 2019;9:8875.
53. Toussaint D, Kuwabara T, Cogan DG. Retinal vascular patterns. II. Human retinal vessels studied in three dimensions. *Arch Ophthalmol*. 1961;65:575–581.
 54. Dubow M, Pinhas A, Shah N, et al. Classification of human retinal microaneurysms using adaptive optics scanning light ophthalmoscope fluorescein angiography. *Invest Ophthalmol Vis Sci*. 2014;55:1299–1309.
 55. Houston WR, Wise GN. Circinate retinopathy. I. *AMA Arch Ophthalmol*. 1957;58:777–782.
 56. Houston WR, Wise GN. Circinate retinopathy. II. *AMA Arch Ophthalmol*. 1957;58:783–796.
 57. Gass JDM. Muller cell cone, an overlooked part of the anatomy of the fovea centralis - Hypotheses concerning its role in the pathogenesis of macular hole and foveomacular retinoschisis. *Arch Ophthalmol*. 1999;117:821–823.
 58. Nag TC, Wadhwa S. Immunolocalisation pattern of complex I-V in ageing human retina: correlation with mitochondrial ultrastructure. *Mitochondrion*. 2016;31:20–32.
 59. Quinn N, Csincsik L, Flynn E, et al. The clinical relevance of visualising the peripheral retina. *Prog Retin Eye Res*. 2019;68:83–109.
 60. Klaassen I, Van Noorden CJ, Schlingemann RO. Molecular basis of the inner blood-retinal barrier and its breakdown in diabetic macular edema and other pathological conditions. *Prog Retin Eye Res*. 2013;34:19–48.
 61. Lieth E, Barber AJ, Xu B, et al. Glial reactivity and impaired glutamate metabolism in short-term experimental diabetic retinopathy. Penn State Retina Research Group. *Diabetes*. 1998;47:815–820.
 62. Attwell D, Buchan AM, Charpak S, Lauritzen M, Macvicar BA, Newman EA. Glial and neuronal control of brain blood flow. *Nature*. 2010;468:232–243.
 63. Simo R, Hernandez C. Novel approaches for treating diabetic retinopathy based on recent pathogenic evidence. *Prog Retin Eye Res*. 2015;48:160–180.
 64. Sohn EH, van Dijk HW, Jiao C, et al. Retinal neurodegeneration may precede microvascular changes characteristic of diabetic retinopathy in diabetes mellitus. *Proc Natl Acad Sci USA*. 2016;113:E2655–2664.
 65. Barber AJ. A new view of diabetic retinopathy: a neurodegenerative disease of the eye. *Prog Neuropsychopharmacol Biol Psychiatry*. 2003;27:283–290.
 66. Curcio CA, Sloan KR, Kalina RE, Hendrickson AE. Human photoreceptor topography. *J Comp Neurol*. 1990;292:497–523.
 67. Yu D-Y, Cringle SJ, Yu PK, Su E-N. Retinal energetics: its critical role in retinal physiology and pathology. *Expert Rev Ophthalmol*. 2011;6:395–399.
 68. Spaide RF. Retinal vascular cystoid macular edema: review and new theory. *Retina*. 2016;36:1823–1842.
 69. Yu DY, Cringle SJ, Su EN. Intraretinal oxygen distribution in the monkey retina and the response to systemic hyperoxia. *Invest Ophthalmol Vis Sci*. 2005;46:4728–4733.
 70. Ahmed J, Braun RD, Dunn R, Jr, Linsenmeier RA. Oxygen distribution in the macaque retina. *Invest Ophthalmol Vis Sci*. 1993;34:516–521.
 71. Yu D-Y, Cringle SJ, Alder VA, Su EN. Intraretinal oxygen distribution in rats as a function of systemic blood pressure. *Am J Physiol*. 1994;36:H2498–H2507.
 72. Liu Z, Tam J, Saeedi O, Hammer DX. Transretinal cellular imaging with multimodal adaptive optics. *Biomed Opt Express*. 2018;9:4246–4262.
 73. Tan PE, Balaratnasingam C, Xu J, et al. Quantitative comparison of retinal capillary images derived by speckle variance optical coherence tomography with histology. *Invest Ophthalmol Vis Sci*. 2015;56:3989–3996.
 74. Chan G, Balaratnasingam C, Xu J, et al. In vivo optical imaging of human retinal capillary networks using speckle variance optical coherence tomography with quantitative clinico-histological correlation. *Microvasc Res*. 2015;100:32–39.